PHYSICAL REVIEW A **79**, 041401(R) (2009)

Effects of electron structure and multielectron dynamical response on strong-field multiphoton ionization of diatomic molecules with arbitrary orientation: An all-electron time-dependent density-functional-theory approach

Dmitry A. Telnov[1,2,*] and Shih-I Chu (朱時宜)[2,3,†]

[1]*Department of Physics, St. Petersburg State University, 198504 St. Petersburg, Russia*

[2]*Center for Quantum Science and Engineering, and Department of Physics, National Taiwan University, Taipei 106, Taiwan*

[3]*Department of Chemistry, University of Kansas, Lawrence, Kansas 66045, USA*

(Received 30 January 2009; published 3 April 2009)

We present a time-dependent density-functional-theory approach for the *ab initio* study of the effect of correlated multielectron responses on the multiphoton ionization (MPI) of diatomic molecules N_2, O_2, and F_2 in intense short laser pulse fields with arbitrary molecular orientation. We show that the contributions of inner molecular orbitals to the total MPI probability can be significant or even dominant over the highest-occupied molecular orbital, depending on detailed electronic structure and symmetry, laser field intensity, and orientation angle.

DOI: 10.1103/PhysRevA.79.041401 PACS number(s): 33.80.Rv, 31.15.ee

Processes involving diatomic molecules in intense laser fields continue attracting much attention and have been a subject of many experimental and theoretical investigations (see, e.g., Ref. [1]). Due to the extra internuclear degree of freedom, the response of molecules to strong fields is considerably more complicated than that of atoms. Recent advances in laser technology and experimental techniques have made possible impressive observations and measurements on diatomic molecules including molecular axis orientation effects, multiple molecular orbital (MO) contributions, electron diffraction, etc. [2–6]. Multiphoton ionization (MPI) is one of the fundamental atomic and molecular processes that takes place in strong laser fields. Recent experiments with diatomic molecules [3,4] were able to perform direct measurements of dependence of the ionization signal on the orientation of the molecular axis with respect to the polarization of the laser field. Thus the theoretical description of the orientation dependence of MPI remains an important and timely task. Traditionally many theoretical studies of MPI processes in molecules are based on the models (molecular Keldysh-Faisal-Reiss (KFR) model [7] and molecular Ammosov-Delone-Krainov (ADK) [8] model which have their origin in earlier works of Keldysh *et al.* [9]). While these models result in rather simple theoretical expressions and are capable of providing some qualitative predictions, they can fail to explain some experimental observations in stronger fields. We note that molecular ADK, KFR, and other simplified models usually deal only with the highest-occupied molecular orbital (HOMO) and neglect the multielectron dynamics of the target molecules. In this Rapid Communication, we extend the time-dependent density-functional theory (TDDFT) [10,11], with proper long-range potential, to an all-electron three-dimensional (3D) *ab initio* study of the MPI of diatomic molecules with arbitrary molecular axis orientation, a subject of much current experimental interest [3–6]. Our calculations show that the contributions of the inner-shell valence MO to MPI signal can be very significant and even dominant over the HOMO contribution, depending upon the target molecule, orientation angle, and the intensity of the laser field, and in general good agreement with most recent experimental results [3,4].

The basic equations of TDDFT are the time-dependent one-electron Kohn-Sham equations for spin orbitals $\psi_{j\sigma}(\boldsymbol{r},t)$ which involve an effective potential $v_{\mathrm{eff},\sigma}(\boldsymbol{r},t)$ (atomic units are used),

$$i\frac{\partial}{\partial t}\psi_{j\sigma}(\boldsymbol{r},t)=\left[-\frac{1}{2}\nabla^2+v_{\mathrm{eff},\sigma}(\boldsymbol{r},t)\right]\psi_{j\sigma}(\boldsymbol{r},t),\quad j=1,2,\ldots,N_\sigma. \tag{1}$$

Here N_σ ($=N_\uparrow$ or $N_\downarrow$) is the total number of electrons for a given spin σ; the total number of electrons in the system is $N=\Sigma_\sigma N_\sigma$. The time-dependent effective potential $v_{\mathrm{eff},\sigma}(\boldsymbol{r},t)$ is a functional of the electron spin densities $\rho_\sigma(\boldsymbol{r},t)$ which are related to the spin orbitals as follows:

$$\rho_\sigma(\boldsymbol{r},t)=\sum_{j=1}^{N_\sigma}|\psi_{j\sigma}(\boldsymbol{r},t)|^2 \tag{2}$$

(the summation includes all spin orbitals with the same spin). The potential $v_{\mathrm{eff},\sigma}(\boldsymbol{r},t)$ can be written in the general form

$$v_{\mathrm{eff},\sigma}(\boldsymbol{r},t)=v_{\mathrm{n}}(\boldsymbol{r})+v_{\mathrm{H}}(\boldsymbol{r},t)+v_{\mathrm{xc},\sigma}(\boldsymbol{r},t)+v_{\mathrm{ext}}(\boldsymbol{r},t), \tag{3}$$

where $v_{\mathrm{n}}(\boldsymbol{r})$ is the electron interaction with the nuclei,

$$v_{\mathrm{n}}(\boldsymbol{r})=-\frac{Z}{|\boldsymbol{R}_1-\boldsymbol{r}|}-\frac{Z}{|\boldsymbol{R}_2-\boldsymbol{r}|} \tag{4}$$

with Z being the nuclear charge (we consider homonuclear diatomic molecules only) and $\boldsymbol{R}_1$ and $\boldsymbol{R}_2$ being the positions of the nuclei (which are assumed to be fixed at their equilibrium positions); $v_{\mathrm{H}}(\boldsymbol{r},t)$ is the Hartree potential due to electron-electron Coulomb interaction,

$$v_{\mathrm{H}}(\boldsymbol{r},t)=\int\frac{\rho(\boldsymbol{r}',t)d^3r'}{|\boldsymbol{r}-\boldsymbol{r}'|}, \tag{5}$$

*telnov@pcqnt1.phys.spbu.ru

†sichu@ku.edu

$$\rho(\boldsymbol{r},t) = \sum_{\sigma} \rho_{\sigma}(\boldsymbol{r},t). \tag{6}$$

In any density-functional calculations, the key role is played by the exchange-correlation (xc) potential $v_{\mathrm{xc},\sigma}(\boldsymbol{r},t)$ which must be a functional of the electron density. The exact form of $v_{\mathrm{xc},\sigma}(\boldsymbol{r},t)$ is unknown. However, high-quality approximations to the xc potential are becoming available. When these potentials, determined by time-independent ground-state density functional theory (DFT), are used along with TDDFT in the electronic structure calculations, both inner shell and excited states can be calculated rather accurately [12]. In the time-dependent calculations, we adopt the commonly used adiabatic approximation, where the xc potential is calculated with the time-dependent density. The adiabatic approximation had many successful applications in the recent studies of atomic and molecular processes in intense external fields [10,12]. In this work, we utilize the following van Leeuwen-Baerends LBα xc potential [13]:

$$v_{\mathrm{xc},\sigma}^{\mathrm{LB}\alpha}(\boldsymbol{r},t) = \alpha v_{\mathrm{x},\sigma}^{\mathrm{LSDA}}(\boldsymbol{r},t) + v_{\mathrm{c},\sigma}^{\mathrm{LSDA}}(\boldsymbol{r},t) - \frac{\beta x_{\sigma}^{2}(\boldsymbol{r},t)\rho_{\sigma}^{1/3}(\boldsymbol{r},t)}{1 + 3\beta x_{\sigma}(\boldsymbol{r},t)\ln\{x_{\sigma}(\boldsymbol{r},t) + [x_{\sigma}^{2}(\boldsymbol{r},t) + 1]^{1/2}\}}. \tag{7}$$

The LBα potential contains two parameters, α and β, which have been adjusted in time-independent DFT calculations of several molecular systems and have the values $\alpha=1.19$ and $\beta=0.01$ [13]. The first two terms in Eq. (7), $v_{\mathrm{x},\sigma}^{\mathrm{LSDA}}$ and $v_{\mathrm{c},\sigma}^{\mathrm{LSDA}}$, are the exchange and correlation potentials within the local spin-density approximation (LSDA). The last term in Eq. (7) is the gradient correction with $x_{\sigma}(\boldsymbol{r}) = |\nabla\rho_{\sigma}(\boldsymbol{r})|/\rho_{\sigma}^{4/3}(\boldsymbol{r})$, which ensures the proper long-range asymptotic behavior $v_{\mathrm{xc},\sigma}^{\mathrm{LB}\alpha} \to -1/r$ as $r \to \infty$. Potential (7) has proved to be reliable in molecular TDDFT studies [11,14]. The correct long-range asymptotic behavior of the LBα potential is crucial in photoionization problems since it allows us to reproduce accurate MO energies and the proper treatment of the molecular continuum.

The potential $v_{\mathrm{ext}}(\boldsymbol{r},t)$ in Eq. (3) describes the interaction with the laser field. Using the dipole approximation and the length gauge, it can be expressed as follows:

$$v_{\mathrm{ext}}(\boldsymbol{r},t) = (\boldsymbol{F}(t)\cdot\boldsymbol{r}). \tag{8}$$

Here $\boldsymbol{F}(t)$ is the electric field strength of the laser field and the linear polarization is assumed. For the laser pulses with the sine-squared envelope, one has

$$\boldsymbol{F}(t) = \boldsymbol{F}_0 \sin^2\frac{\pi t}{T}\sin\omega_0 t, \tag{9}$$

where T and ω_0 denote the pulse duration and the carrier frequency, respectively, and F_0 is the peak field strength. In our calculations, we used the laser wavelength 800 nm ($\omega_0=0.0569$ a.u.) and the sine-squared envelope with 20 optical cycles.

Before solving the Cauchy problem for the set of equations (1), one has to prepare the initial Kohn-Sham spin orbitals $\psi_{j\sigma}(\boldsymbol{r},t=0)$. This problem is solved within the framework of the time-independent DFT, using the same LBα xc potential and appropriate self-consistent procedure. In the calculations, we used the experimental values of the equilibrium internuclear separations [15] (2.074 a.u. for N_2, 2.282 a.u. for O_2, and 2.668 a.u. for F_2). In Table I, we summarize the energies for the spin orbitals that have a significant contribution to MPI and the corresponding experimental vertical ionization potentials. While N_2 and F_2 represent the spin-compensated case with the same orbital energies for both spin projections, O_2 is a spin-polarized system where the spin orbital energies depend on the spin. The agreement between the calculated and experimental values is fairly good, particularly for N_2 molecule.

TABLE I. (A) Absolute values of spin orbital energies of diatomic molecules of present DFT calculations (eV). (B) Experimental vertical ionization potentials (eV).

Molecule	Spin orbital	A	B
N_2	$2\sigma_u$	18.5	18.7 (Ref. [16])
	$1\pi_u$	16.9	17.2 (Ref. [16])
	$3\sigma_g$ (HOMO)	15.5	15.6 (Ref. [16])
O_2	$3\sigma_g\downarrow$	18.3	18.2 (Ref. [17])
	$1\pi_u\downarrow$	17.4	16.7 (Ref. [17])
	$1\pi_g\uparrow$ (HOMO)	12.8	12.3 (Ref. [17])
F_2	$3\sigma_g$	21.9	21.0 (Ref. [18])
	$1\pi_u$	19.2	19.0 (Ref. [18])
	$1\pi_g$ (HOMO)	16.0	15.7 (Ref. [18])

The set of equations (1) is solved by means of the time-dependent generalized pseudospectral method in prolate spheroidal coordinates [19]. The details of the present computational procedure will be described elsewhere. Here we outline some aspects relevant to the definition of the ionization probability. When solving Eq. (1), the radial coordinate is restricted to the domain from 0 to 60 a.u.; between 40 and 60 a.u. we apply an absorber which smoothly brings down the wave function for each spin orbital without spurious reflections. Absorbed parts of the wave packet localized beyond 40 a.u. describe unbound states populated during the ionization process. Because of the absorber, the normalization integrals of the wave functions $\psi_{j\sigma}(\boldsymbol{r},t)$ decrease in time. Calculated after the pulse, they give the survival probabilities $P_{j\sigma}^{(\mathrm{s})}$ for each spin orbital,

$$P_{j\sigma}^{(\mathrm{s})} = \int d^3r |\psi_{j\sigma}(\boldsymbol{r},T)|^2. \tag{10}$$

Then one can define the spin orbital ionization probabilities $P_{j\sigma}^{(i)}$ as

$$P_{j\sigma}^{(\mathrm{i})} = 1 - P_{j\sigma}^{(\mathrm{s})}. \tag{11}$$

However, the total ionization probability of the molecule $P^{(\mathrm{i})}$ is not equal to the sum of the spin orbital probabilities. The molecule survives the laser pulse (does not get ionized) if (and only if) every spin orbital survives as well. Then the

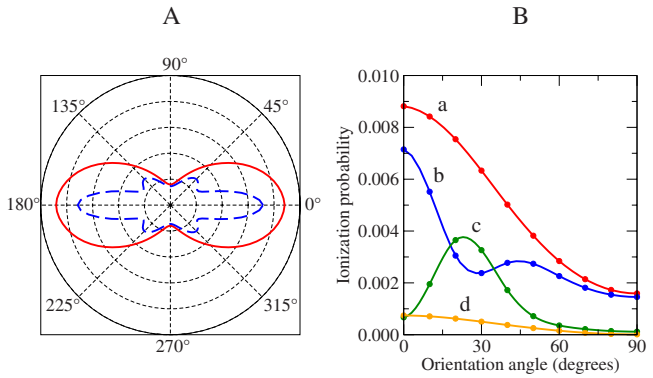

FIG. 1. (Color online) MPI probability of N_2 molecule for the peak intensity of 1×10^{14} W/cm^2. Panel A: polar plot of total probability (solid red line) and HOMO contribution (dashed blue line). Panel B: total and orbital MPI probabilities: (a) total probability, (b) $3\sigma_g$ (HOMO) probability, (c) $1\pi_u$ probability, and (d) $2\sigma_u$ probability.

total survival probability $P^{(s)}$ can be calculated as

$$P^{(s)} = \prod_{j\sigma} P^{(s)}_{j\sigma} = \prod_{j\sigma} (1 - P^{(i)}_{j\sigma}). \tag{12}$$

Accordingly, the total ionization probability can be written as

$$P^{(i)} = 1 - P^{(s)} = 1 - \prod_{j\sigma} (1 - P^{(i)}_{j\sigma}). \tag{13}$$

The total ionization probability as defined by Eq. (13) reduces to the sum of the spin orbital probabilities only in the limit of the weak laser field (small $P^{(i)}_{j\sigma}$).

We have computed the orientation-dependent MPI probabilities for N_2 and O_2 molecules at the peak intensity of 1×10^{14} W/cm^2. The orientation dependence of the total MPI probabilities for N_2 (Fig. 1) and O_2 (Fig. 2) is in good accord with the experimental observations [3,4] for these molecules and reflects the symmetries of their HOMO. For N_2, the maximum corresponds to the parallel orientation, and for O_2 it is located at about 40°. However, while for O_2 the total probability is clearly dominated by the HOMO contribution, for N_2 multielectron effects are more important, particularly at intermediate orientation angles. Between 18° and 35°, the orbital probability of HOMO−1 ($1\pi_u$) is larger than that of HOMO ($3\sigma_g$). Despite the orbital probabilities have local minima and maxima, the total probability shows monotonous dependence on the orientation angle. An analysis of spin orbital energies (Table I) can help to understand the relative importance of MPI from inner shells in N_2 compared to that in O_2. The smaller the ionization potential of the electronic shell, the easier it can be ionized. That is why HOMO is generally expected to give the main contribution to the MPI probability. However, in N_2 the ionization potential of HOMO−1 is quite close to that of HOMO (the difference between the calculated values is 1.4 eV), and in the strong enough laser field (1×10^{14} W/cm^2) both shells show comparable ionization probabilities. At the same time, the gap between the energies of HOMO and HOMO−1 in O_2 is much larger (our calculation gives the value of 4.6 eV), and HOMO contribution to the MPI probability remains dominant for the laser pulse with the peak intensity of 1×10^{14} W/cm^2. At higher intensities the situation may change, as suggested by the next example of F_2 molecule.

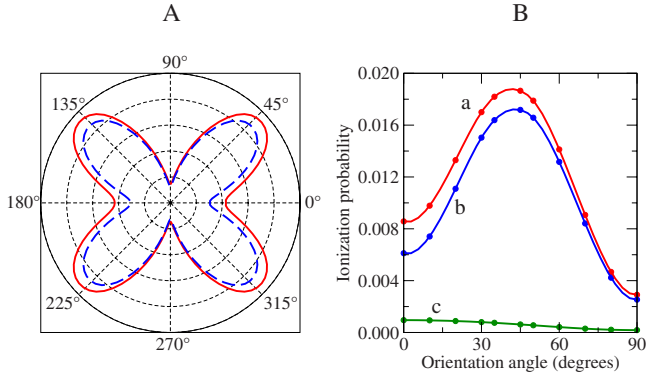

FIG. 2. (Color online) MPI probability of O_2 molecule for the peak intensity of 1×10^{14} W/cm^2. Panel A: polar plot of total probability (solid red line) and HOMO contribution (dashed blue line). Panel B: total and orbital MPI probabilities: (a) total probability, (b) $1\pi_g\uparrow$ (HOMO) probability, and (c) $1\pi_u\downarrow$ probability.

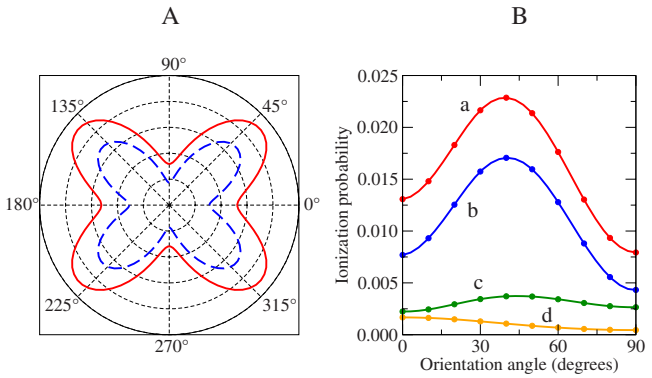

FIG. 3. (Color online) MPI probability of F_2 molecule for the peak intensity of 2×10^{14} W/cm^2. Panel A: polar plot of total probability (solid red line) and HOMO contribution (dashed blue line). Panel B: total and orbital MPI probabilities: (a) total probability, (b) $1\pi_g$ (HOMO) probability, (c) $1\pi_u$ probability, and (d) $3\sigma_g$ probability.

For F_2, we present here the results for the peak intensities of 2×10^{14} W/cm^2 (Fig. 3) and 1×10^{15} W/cm^2 (Fig. 4). At the lower intensity of 2×10^{14} W/cm^2, the pattern for the orientation dependence of MPI in F_2 resembles that in O_2, with the maximum pointing at 40°. The HOMO−1 contribution is somewhat larger than that in O_2, and this is well explained by the smaller gap between the HOMO and HOMO−1 energies (3.2 eV). At the higher intensity of 1×10^{15} W/cm^2, the picture changes dramatically. First, the orientation angle dependence of the total MPI probability becomes almost isotropic. Second, the contribution from HOMO−1 exceeds that from HOMO at all angles, and for small angles (0° to 18°) both HOMO and HOMO−1 are dominated by HOMO−2 ($3\sigma_g$). This significant and interesting phenomenon of orbital switching with increasing intensity was reported previously for the parallel orientation of the molecular axis [11].

In summary, we have presented an *ab initio* all-electron

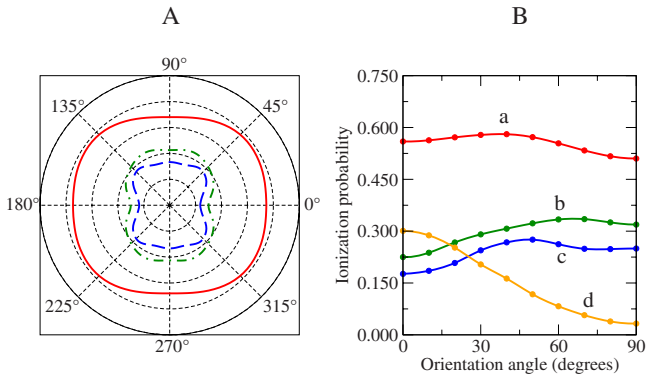

FIG. 4. (Color online) MPI probability of F_2 molecule for the peak intensity of 1×10^{15} W/cm^2. Panel A: polar plot of total probability (solid red line), HOMO contribution (dashed blue line), and HOMO−1 contribution (dot-and-dash green line). Panel B: total and orbital MPI probabilities: (a) total probability, (b) $1\pi_u$ (HOMO−1) probability, (c) $1\pi_g$ (HOMO) probability, and (d) $3\sigma_g$ probability.

TDDFT investigation of the role of electron structure and multielectron response to the strong-field MPI of several diatomic molecules with arbitrary orientation of the molecular axis. We have shown that for 800 nm laser pulses with the peak intensity of 1×10^{14} W/cm^2 the inner-shell contributions to the MPI probability are quite significant for N_2 molecule, particularly at intermediate angles, while for O_2 the HOMO contribution is still dominant. This observation is in agreement with the electronic structure and positions of the spin orbital energy levels for these species. Our calculations performed on F_2 molecule at the peak intensities of 2×10^{14} and 1×10^{15} W/cm^2 show the trend which may be expected on other diatomic molecules as well. With increasing intensity of the laser field, the effect of the inner-shell electrons on MPI becomes more important, and orbital switching may occur: the contributions of spin orbitals with larger ionization potentials exceed those of spin orbitals with smaller ionization potentials. Since several spin orbitals possessing different symmetries make substantial contributions to MPI, the dependence of the total MPI probability on the orientation angle becomes more isotropic. In conclusion, our study provides numerical results and physical insights for the understanding of the origin of the orbital switching phenomenon recently observed in several experiments which cannot be explained by simplified models.

This work was partially supported by the Chemical Sciences, Geosciences and Biosciences Division of the Office of Basic Energy Sciences, Office of Sciences, Department of Energy, by the National Science Foundation. We also would like to acknowledge the partial support of National Science Council of Taiwan (Grant No. 97-2112-M-002-003-MY3) and National Taiwan University (Grant No. 97R0066).

[1] J. H. Posthumus, Rep. Prog. Phys. **67**, 623 (2004).
[2] E. Wells, M. J. DeWitt, and R. R. Jones, Phys. Rev. A **66**, 013409 (2002).
[3] D. Pavicic, K. F. Lee, D. M. Rayner, P. B. Corkum, and D. M. Villeneuve, Phys. Rev. Lett. **98**, 243001 (2007).
[4] I. Thomann *et al.*, J. Phys. Chem. A **112**, 9382 (2008).
[5] M. Meckel *et al.*, Science **320**, 1478 (2008).
[6] B. K. McFarland *et al.*, Science **322**, 1232 (2008).
[7] J. Muth-Böhm, A. Becker, and F. H. M. Faisal, Phys. Rev. Lett. **85**, 2280 (2000).
[8] X. M. Tong, Z. X. Zhao, and C. D. Lin, Phys. Rev. A **66**, 033402 (2002).
[9] L. V. Keldysh, Zh. Eksp. Teor. Fiz. **47**, 1945 (1964) [Sov. Phys. JETP **20**, 1307 (1965)]; F. H. M. Faisal, J. Phys. B **6**, L89 (1973); H. R. Reiss, Phys. Rev. A **22**, 1786 (1980).
[10] S. I. Chu, J. Chem. Phys. **123**, 062207 (2005).
[11] X. Chu and Shih-I Chu, Phys. Rev. A **70**, 061402(R) (2004).
[12] *Time-Dependent Density Functional Theory*, edited by M. A. L. Marques, C. A. Ullrich, F. Nogueira, A. Rubio, K. Burke, and E. K. U. Gross (Springer, Berlin, 2006).
[13] P. R. T. Schipper *et al.*, J. Chem. Phys. **112**, 1344 (2000).
[14] J. Heslar *et al.*, Int. J. Quantum Chem. **107**, 3159 (2007).
[15] K. P. Huber and G. Herzberg, *Molecular Spectra and Molecular Structure IV: Constants of Diatomic Molecules* (Reinhold, New York, 1979).
[16] A. Lofthus and P. H. Krupenie, J. Phys. Chem. Ref. Data **6**, 113 (1977).
[17] P. Baltzer, B. Wannberg, L. Karlsson, M. Carlsson Gothe, and M. Larsson, Phys. Rev. A **45**, 4374 (1992).
[18] A. B. Cornford *et al.*, J. Chem. Phys. **54**, 2651 (1971).
[19] D. A. Telnov and Shih-I Chu, Phys. Rev. A **76**, 043412 (2007).